Journal of Orthopaedic Surgery and Research

RESEARCH

Open Access

Insights into the potential role of BMSCs-exo delivered USP14 on SIRT1 deubiquitination in Staphylococcus aureus-induced model of osteomyelitis

Jun Yu[1], Ming Yang[2], Yun Jin[1], Kaijie Yang[1] and Haibo Yang[1*]

Abstract

Osteomyelitis resulting from a traumatic fracture is a recurrent and difficult-to-treat bone infection. Ubiquitin-specific protease 14 (USP14), a deubiquitinating enzyme, and Sirtuin-1 (SIRT1), an NAD+-dependent deacetylase, both play critical roles in regulating cellular processes, including inflammation. It has been discovered that exosomes originated from bone marrow mesenchymal stem cells (BMSCs-exo) can promote the repair and regeneration of bone fractures. In this study, we aimed to investigate the role of BMSCs-exo in osteoblast differentiation in osteomyelitis and the related molecular mechanisms. MC3T3-E1 cells induced with S. aureus were used as an in vitro model of osteomyelitis. BMSCs-exo were isolated and characterized using ultracentrifugation, transmission electron microscopy (TEM), and Western blot. RT-qPCR, Western blot, CCK-8, ALP staining, ELISA, and CO-IP were utilized to evaluate USP14 and SIRT1 levels, the osteogenic differentiation ability of MC3T3-E1 cells, and the deubiquitination level of SIRT1. Low expression of USP14 and SIRT1 was observed in the bone tissue of osteomyelitis patients. BMSCs-exo could upregulate the expression of USP14 and promote the expression of SIRT1 protein in the cell model of osteomyelitis. In addition, BMSCs-exo reduced the levels of inflammatory factors TNFα and IL-6, enhanced cell viability, promoted the expression of osteogenic differentiation markers RUNX2 and OCN in MC3T3-E1 cells, and improved cell osteogenic capacity. However, these trends were significantly reversed in MC3T3-E1 cells following treatment with BMSCs-exo transfected with si-USP14. Furthermore, knockdown of USP14 promoted SIRT1 ubiquitination and degradation, the process that was reversed by the proteasome inhibitor MG132, whereas USP14 overexpression inhibited SIRT1 ubiquitination. In MC3T3-E1 cells infected with S. aureus, BMSCs-exo delivers USP14, which may enhance SIRT1 deubiquitination and increase SIRT1 protein activity. This process inhibits inflammation and promotes osteogenesis, warranting further investigation into its mechanisms and in vivo efficacy.

Keywords BMSCs, Exosomes, USP14, SIRT1, Osteoblast differentiation, Osteomyelitis

*Correspondence:
Haibo Yang
boneyanghaibo@163.com
[1]Orthopaedic Trauma Department, General Hospital of Ningxia Medical University, 804 Shengli South Street, Xingqing District, Yinchuan City, Ningxia 750001, China
[2]Emergency Department, People's Hospital of Ningxia Hui Autonomous Region, Ningxia, China

Introduction

Post-fracture osteomyelitis is a challenging complication occurring in 1–2% of limb fractures, often recurring and difficult to treat [1]. With the continuous aging population, the number of patients with traumatic osteomyelitis caused by fractures is also increasing, imposing a heavy economic burden on patients' families and society. Studies have shown that the pathological characteristic of traumatic osteomyelitis is persistent inflammatory stimulation, leading to scar formation and necrosis in surrounding tissues [2]. Research has also indicated that, in addition to the EGF signaling pathway and static magnetic fields [3, 4], pro-inflammatory mediators secreted during osteomyelitis are some of the factors that regulate osteoblast differentiation, leading to increased bone loss and fracture risk in fracture patients, as well as significantly prolonged treatment time [5–7]. Therefore, exploring the pathological mechanisms of osteomyelitis and inhibiting inflammation may be an important strategy for treating osteomyelitis.

Staphylococcus aureus (S. aureus) is one of the most common pathogenic bacteria, and the infections it causes lead to osteomyelitis [8]. The MC3T3-E1 cell line, derived from mouse calvarial osteoprogenitor cells, possesses the majority of the molecular features of osteocytes and is widely used to simulate the osteogenic process in bone tissue [9]and its response to bacterial infections [10]. Previous studies have shown that co-culturing MC3T3-E1 cells with S. aureus can establish an in vitro model of osteomyelitis [11, 12]. Therefore, this study utilized a co-culture system of MC3T3-E1 cells and S. aureus to construct an osteomyelitis model, aiming to provide new insights into treatment strategies for osteomyelitis.

Bone marrow mesenchymal stem cells (BMSCs) have been proven to be an effective means for bone tissue repair and regeneration, including osteoporosis and fractures [13–16]. In recent years, multiple studies have shown that BMSCs mainly promote the healing of bone injury tissues through paracrine secretion during the repair process [17, 18]. Exosomes are small vesicles derived from within cells and secreted outside the cell through exocytosis, acting on target cells. They contain small molecule miRNAs and biologically active proteins that play a role in information transmission [19]. Studies have confirmed that exosomes derived from bone marrow mesenchymal stem cells (BMSCs-exo) play important roles in osteoblast differentiation, regulation of tissue microenvironment, anti-inflammatory effects, and anti-rheumatic effects [20]. BMSCs-exo can reverse osteoblast differentiation and improve fracture healing caused by obesity [21]. BMSCs-exo promotes the polarization of M1-type macrophages to M2-type by increasing the expression of TUC339, inhibits inflammation, and promotes chondrocyte activity, thereby improving osteoarthritis [22]. However, the therapeutic effect of BMSCs-exo on osteomyelitis and its related molecular mechanisms are currently unclear.

The ubiquitin-proteasome system (UPS) is an ATP-dependent protein selective degradation system within cells. It primarily regulates various biological functions such as inflammation, signal transduction, and immune response by degrading ubiquitinated proteins within the cell [23]. Ubiquitin-specific protease 14 (USP14), belonging to the cysteine hydrolase family, is the only deubiquitinating enzyme located on the 19 S proteasome within UPS, regulating proteasome activity [24]. Recent studies have found that USP14 plays an important role in disease development by regulating inflammatory responses through deubiquitination [25]. In osteoarthritis, USP14 promotes the deubiquitination and degradation of IκBα in bone, enhancing NF-κB activation and modulating the dedifferentiation of chondrocytes stimulated by inflammatory factors [26]. However, it is currently unclear whether USP14 participates in osteomyelitis by regulating inflammatory responses.

Sirtuin 1 (SIRT1), a major member of the sirtuin family, is a highly conserved NAD-dependent deacetylase that plays a role in regulating cell apoptosis, lipid metabolism, oxidative stress, and inflammation [27, 28]. Research has emphasized the important role of SIRT1 in bone injury repair [29, 30]. There are relatively few reports on the involvement of SIRT1 in the progression of osteomyelitis. However, recent findings indicate that resveratrol induced SIRT1 and PGC-1α secretion in LPS-treated MC3T3-E1 cells, further improving mitochondrial function to mitigate the inhibition of osteoblast differentiation by lipopolysaccharides (LPS) [31]. Nevertheless, the role of SIRT1 in regulating inflammation and its related mechanisms in osteomyelitis remains uncertain.

This study seeks to elucidate the significant role of BMSCs-exo in osteomyelitis and explore its potential mechanism in osteoblast differentiation. This study provides potential targets for fracture repair.

Materials and methods

Clinical samples

We recruited 10 patients with combined osteomyelitis fractures and 10 patients with healthy fractures caused by trauma. Bone tissue samples were collected from all participants and frozen in an 80 ℃ refrigerator for further analysis. This study was approved by the Ethics Committee of General Hospital of Ningxia Medical University (approved number: KYLL-2023-0310). Furthermore, the study was conducted in strict accordance with the Declaration of Ethical Principles of Medical Research Involving Human Subjects in Helsinki. All the participants provided written informed consent.

Cell culture and S. aureus infection

This study utilized Mouse BMSCs (CP-M131; Procell Life Science & Technology Co., Ltd., China) and MC3T3-E1 cells obtained from the American Type Culture Collection (ATCC, Rockville, MD, USA) to investigate the effect of BMSCs-exo on an osteomyelitis model induced by S. aureus.

For BMSCs, cells were seeded at a density of 1×10^5 cells per well in 6-well plates and cultured in DMEM medium (2 ml/well, catalog number 430–2100, Gibco, Grand Island, NY, USA) under standard conditions (37 °C, 5% CO_2). Upon reaching 80-90% confluence, the cells were passaged, and the third passage was used for subsequent experiments. During the culture period, no spontaneous differentiation was observed. Corresponding experiments were conducted using the BMSCs osteogenic differentiation kit (Catalog number CHEM-200004/5/6, Shanghai Linmeng Biotechnology, China), as well as alizarin red S and oil red O staining.

MC3T3-E1 cells were seeded at a density of 3×10^4 cells per well in 6-well plates and cultured under 5% CO2 at 37 °C in minimum essential medium (alpha-MEM; catalog number 12571063, Gibco, Grand Island, NY) supplemented with 10% fetal bovine serum (FBS, catalog number 26140095, Gibco), a 1% antibiotic cocktail (penicillin G sodium, streptomycin sulfate; catalog number 15140122, Gibco), and 1% L-glutamine (catalog number G7513, Sigma Aldrich). The medium was replaced every 48 h. When cells reached confluence, they were treated with trypsin, and only cells at passages 12 to 15 were utilized.

The S. aureus infection of MC3T3-E1 cells was performed according to previously established protocols [32], briefly, S. aureus strain 6850 (53657; ATCC, Manassas, VA) was first cultured overnight in BBL Trypticase Soy Broth (TSB; BD Biosciences, Franklin Lakes, NJ) at 37 °C with constant shaking, followed by an additional incubation for 3 h at the same temperature to reach the exponential growth phase. Next, the bacterial suspension was collected by centrifugation (3,000 rpm for 10 min), washed three times with phosphate-buffered saline (PBS) (catalog number 18912014, Gibco), and resuspended in PBS, adjusted to McFarland standard 6 to ensure accurate CFU/ml. Then, this prepared Staphylococcus aureus strain 6850 was used to infect MC3T3-E1 cells at a multiplicity of infection of 100. After incubating at 37 °C for 21 days, the MC3T3-E1 cells were washed with PBS and treated with 20 mg/mL lysostaphin (catalog number L7386, Sigma) for 30 min to remove extracellular bacteria adhering to the cells. Fresh medium was then added to continue the culture.

Table 1 Cell grouping 1

In order to explore the impacts of BMSCs-exo on osteoblasts	
Group Label	**Description**
Control	MC3T3-E1 cells cultured in standard medium without any additional treatment
S. aureus	MC3T3-E1 cells cultured with S. aureus alone
Exo	MC3T3-E1 cells cultured with BMSCs-exo alone
S. aureus + Exo	MC3T3-E1 cells co-cultured with both S. aureus and BMSCs-exo
S. aureus + USP14 Exo	MC3T3-E1 cells treated with S. aureus and then co-cultured with BMSCs-exo overexpressing USP14
S. aureus + si-USP14 Exo	MC3T3-E1 cells treated with S. aureus and then co-cultured with BMSCs-exo transfected with si-USP14

Cell transfection

For both BMSCs and MC3T3-E1 cells, we utilized the overexpression plasmid USP14 (OE-USP14) (GenePharma, Shanghai, China) and small interfering RNA targeting USP14 (si-USP14) (from Dharmacon (Chicago, IL, USA), for USP14 overexpression and knockdown, respectively. Cells were seeded at 5×10^5 cells/well in 6-well plates and transfected when they reached 70–80% confluence. For overexpression, 2 μg of plasmid DNA was mixed with Lipofectamine 2000 (catalog number 11668-019, Invitrogen, USA) in Opti-MEM (catalog number 31985070, Gibco) and added to cells for 48 h. For knockdown, 50 nM si-USP14 was similarly transfected using Lipofectamine 2000. The sequence for si-USP14 was 5'-AGAAATGCCTTGTATATCATT-3'. Transfected cells were then analyzed by reverse transcription polymerase chain reaction (RT-qPCR) or Western blot after 48 h.

Cell grouping

For all experiments involving BMSCs-exo, a fixed concentration of approximately 20 μg/mL was used. In order to explore the impacts of BMSCs-exo on osteoblasts, MC3T3-E1 cells were cultivated in medium containing only BMSCs-exo or S. aureus, or cultured in medium containing MC3T3-E1 with BMSCs-exo added after treatment with S. aureus. These groups were divided into S. aureus groups, Exo groups, and S. aureus + Exo groups. To evaluate the effects of BMSCs-exo on osteoblasts through USP14, BMSCs were first transfected with either the OE-USP14 or si-USP14 using liposomes. The exosomes secreted by these transfected BMSCs were then collected and co-cultured with S. aureus-treated MC3T3-E1 cells. These groups were labeled as S. aureus + USP14 Exo groups and S. aureus + si-USP14 Exo groups. For details, see the Table 1.

To investigate the mechanism of action of USP14 in MC3T3-E1 cells, we transfected overexpression negative control (OE-NC), OE-USP14, small interfering RNA negative control (si-NC), or si-USP14 was transfected into MC3T3-E1 cells using of liposomes. Some experiments were also combined with MG132 treatment (a

proteasome inhibitor, (10 μM; M7449, Sigma-Aldrich). When investigating the effects of si-USP17, the groups were divided into Control, si-USP14, MG132, and si-USP14 + MG132. For OE-USP17, the groups were divided into NC group and USP14 group. For details, see the Tables 2 and 3.

Table 2 Cell grouping 2

To investigate the mechanism of action of USP14 in MC3T3-E1 cells (si-USP14)	
Group Label	**Description**
Control	MC3T3-E1 cells cultured in standard medium without any additional treatment
si-USP14	MC3T3-E1 cells transfected with si-USP14
MG132	MC3T3-E1 cells treated with the proteasome inhibitor MG132
si-USP14 + MG132	MC3T3-E1 cells transfected with si-USP14 and subsequently treated with MG132

Table 3 Cell grouping 3

To investigate the mechanism of action of USP14 in MC3T3-E1 cells (OE-USP14)	
Group Label	**Description**
NC	MC3T3-E1 cells transfected with OE-NC
USP14	MC3T3-E1 cells transfected with OE-USP14

Isolation and identification of BMSCs-exo

To isolate and characterize exosomes derived from BMSCs for their potential therapeutic effects on osteomyelitis induced by S. aureus. BMSCs were seeded at a density of 5×10^5 cells per well in 6-well plates and cultured in DMEM medium (catalog number 430–2100, Gibco, Grand Island, NY, USA). After reaching the desired confluence, the supernatant was collected for exosome isolation. The collected supernatant (20 mL) was initially centrifuged at 350 g for 10 min to remove cells and large debris. The supernatant was then transferred to a new centrifuge tube and centrifuged at 2000 g for 30 min to pellet dead cells and larger cell fragments. Exosomes were precipitated from the clarified supernatant using ExoQuick-TC (System Biosciences Inc., Palo Alto, CA) at a 1:5 reagent-to-supernatant ratio. The mixture was incubated at 4 °C for 12 h and then centrifuged at 1,500×g for 30 min to pellet the exosomes. The exosome pellet was resuspended in PBS and subsequently characterized by transmission electron microscopy (TEM) and Western blot analysis. After characterization, the exosomes were stored at -80 °C.

TEM analysis of BMSCs-exo

To characterize the morphology and size of BMSCs-exo using TEM, the mixed BMSCs-exo (20 μg in 20 μL) were dropped onto a carbon support film copper grid and left to stand at 25℃ for 5 min. Subsequently, the added 3% phosphotungstic acid (catalog number: HT152, Sigma-Aldrich) was addded for 5 min of negative staining, The remaining liquid was removed using filter paper, and the grid was left to dry in the air. The grid was observed and photographed under the TEM (JEM-F200, Japan).

Alizarin red S staining

To evaluate the osteogenic differentiation potential of BMSCs using Alizarin Red S staining, BMSCs were seeded at 5×10^4 cells/well in 6-well plates. Upon reaching 80% confluence, cells were induced with the osteogenic differentiation medium provided by the BMSC Osteogenic Differentiation Kit (catalog number CHEM-200004/5/6, Shanghai Linmeng Biotechnology, China) according to the manufacturer's instructions for 21 days, with medium changes every 3 days. For staining, cells were fixed with 4% paraformaldehyde (catalog number 158127, Sigma-Aldrich) for 15 min and washed with PBS (catalog number 18912014, Gibco). Cells were then stained with 1% Alizarin Red S solution (catalog number 02100375, MP Biomedicals, Thermo Fisher Scientific) (pH 4.2) for 15 min at room temperature. After staining, cells were washed with distilled water until the background was clear. Mineralized nodules were observed and photographed under a microscope (Olympus, BX53, Japan).

Oil red O staining

To evaluate the adipogenic differentiation potential of BMSCs using Oil Red O staining, BMSCs were seeded at 5×10^4 cells/well in 6-well plates. Upon reaching 80% confluence, cells were induced with adipogenic medium (DMEM/F12 supplemented with 10% FBS, 1 μM dexamethasone, 0.5 mM IBMX, 10 μg/mL insulin, and 100 μM indomethacin) for 14 days, with medium changes every 3 days. For staining, cells were fixed with 4% paraformaldehyde (catalog number 158127, Sigma-Aldrich) for 15 min and washed with PBS (catalog number 18912014, Gibco). Cells were rinsed briefly with 60% isopropanol (Sigma-Aldrich) and then stained with freshly prepared Oil Red O solution (in 60% isopropanol, Sigma) for 10 min at room temperature. After staining, cells were washed with distilled water until the background was clear. Lipid droplets were observed and photographed under a microscope (Olympus, BX53, Japan).

Cell counting Kit-8 (CCK-8) assay

To evaluate the cell proliferation rate of MC3T3-E1 cells under different treatments using the CCK-8 assay, MC3T3-E1 cells from each group were gathered and placed in 96-well plates according to the density of 2×10^3

cells per well. The cells were incubated for 48 h until they reached 80% confluence. Subsequently, 20 μL of CCK-8 solution (catalog number CK-04, DOJINDO, Kumamoto, Japan) was added to each well, and the plate was incubated for an additional 2 h in the incubator. The absorbance at 450 nm wavelength of each well was measured using an enzyme immunoassay analyzer (Multiskan FC, ThermoFisher, USA).

ALP staining

To assess the osteogenic differentiation of MC3T3-E1 cells, ALP staining was performed. Cells were seeded at 5×10^4 cells/well in 6-well plates and cultured in an osteogenic differentiation medium using the BMSC osteogenic differentiation kit (catalog number CHEM-200004/5/6, Shanghai Linmeng Biotechnology, China) for 7 days. During the culture period, no spontaneous differentiation was observed. Post-culture, cells were fixed with 4% paraformaldehyde (catalog number 158127, Sigma-Aldrich) for 15 min and washed with PBS (catalog number 18912014, Gibco). Cells were then stained with BCIP/NBT substrate solution (catalog number B5655, Sigma) for 30 min at room temperature. For observation, the stained cells were visualized and photographed under a microscope (Olympus, BX53, Japan).

Enzyme-linked immunosorbent (ELISA) assay

To assess the levels of IL-6 and TNF-α in the supernatant of cultured MC3T3-E1 cells from each group, ELISA assay was performed. Cells were initially seeded at a density of 2×10^5 cells per well in 24-well plates. Cells were then treated according to their respective experimental conditions for a duration of 48 h. After treatment, the supernatant was collected for ELISA analysis. The levels of IL-6 (catalog number PI330, Beyotime, Shanghai, China) and TNF-α (catalog number PT518, Beyotime, Shanghai, China) were measured using ELISA kits. The absorbance of each well was measured using an enzyme.

Reverse transcription polymerase chain reaction (RT-qPCR)

The purpose of conducting this test was to determine the expression levels of USP14 and SIRT1 in cells, pulverized bone samples, and exosomes from each experimental group. Total RNA was extracted from cells and pulverized bone samples using Trizol reagent (catalog number: 15596026, Invitrogen, Carlsbad, CA, USA), and, exosome RNA extraction was conducted using the SeraMirTM Exosome RNA Extraction Kit (System Biosciences, USA) after isolating exosomes. The concentration and quality of RNA were measured using a NanoDrop spectrophotometer (ND-100, Thermo). RNA was reverse transcribed into cDNA according to the instructions of the reverse transcription kit (catalog number 4368814, Applied Biosystems, USA). Fluorescent quantitative PCR amplification was performed using cDNA as the template. The primer sequences were as shown in Table 4. The PCR reaction conditions were as follows: 95℃ for 5 min, 95℃ for 5 s, 60℃ for 20 s, 72℃ for 30 s, for a total of 30 cycles. The relative expression levels of USP14 and SIRT1 were calculated using the $2^{-\Delta\Delta Ct}$ method.

Table 4 RT-qPCR sequences

Genes	Forward(5′-3′)	Reverse(5′-3′)
USP14	CGGGATCCGCCACCATGCCGCTC-TACTCCGTTAC	CCGCTCGAG-GCCACCCT-GTTCACTTTCCTCTTC-CA
SIRT1	TAGCCTTGTCAGATAAGGAAGGA	ACAGCTTCACAGT-CAACTTTGT
β-actin	ACAGGATGCAGAAGGAGATTAC	ACAGTGAGGCCAG-GATAGA

Western blot

The purpose of conducting this test was to analyze the expression levels of USP14, SIRT1, RUNX2, OCN, CD9, CD63, TSG101, Calnexin, and β-actin in MC3T3-E1 cells, bone tissue, and exosomes from each experimental group. MC3T3-E1 cells, bone tissue, and exosomes were collected from each experimental group. For cells and bone tissues, the latter required a pre-processing step due to its dense structure. Bone samples were first pulverized under liquid nitrogen conditions to create a fine powder. This bone powder was then resuspended in an appropriate volume of ice-cold RIPA lysis buffer (catalog number 9806, Cell Signaling Technology) supplemented with protease and phosphatase inhibitors (catalog number 5892791001, Millipore Sigma). Both cell lysates and bone tissue suspensions underwent rigorous vortexing, sonication on ice, and centrifugation at 12,000 rpm for 20 min at 4 °C. The supernatants containing the extracted proteins were collected. Exosome samples were lysed by adding an appropriate volume of RIPA buffer (20 μg of BMSCs-exo per 20 μL of RIPA buffer). All samples were subjected to thorough shaking, ultrasonication, and centrifugation at 12,000 rpm for 20 min at 4 °C. The total protein content of the samples was determined using the BCA method (catalog number 23225, Thermo Fisher Scientific, USA). Then, equal amounts of protein (30 μg) from each sample were mixed with 5× loading buffer and boiled for 5 min to denature the proteins. Subsequently, 15 μl of the samples were taken and separated by 10% SDS-PAGE, followed by transfer to a membrane. The membrane was blocked with 4% BSA (catalog number A7906, Sigma-Aldrich) for a period of 1 h, then incubated with various antibodies overnight at 4 °C: USP14 (1:1000, catalog number ab192618, Abcam, Shanghai, China), SIRT1 (1:1000, catalog number ab189494, Abcam, Shanghai, China), RUNX2 (1:1000, catalog number ab236639,

Abcam, Shanghai, China), OCN (1:1000, catalog number ab93876, Abcam, Shanghai, China), CD9 (1:1000, catalog number ab307085, Abcam, Shanghai, China), CD63 (1:1000, catalog number ab315108, Abcam, Shanghai, China), TSG101 (1:1000, catalog number ab125011, Abcam, Shanghai, China), Calnexin (1:1000, catalog number ab22595, Abcam, Shanghai, China), and β-actin (1:200, catalog number ab5694, Abcam, Shanghai, China). HRP-labeled goat anti-rabbit IgG (1:2000, catalog number ab6721, Abcam) was then added and incubated for 1 h at 4 °C. Protein expression levels were quantified by imaging the membranes using an Amersham Imager 600 (GE Healthcare, Chicago, IL, USA). ImageJ software (version 1.53, NIH, USA) was used to analyze the intensity of the bands. Specifically, the integrated density of each band was measured and normalized to the corresponding β-actin band as an internal control. The relative expression levels were calculated as the ratio of the target protein's integrated density to that of β-actin.

Co-Immunoprecipitation (Co-IP) assay

The purpose of conducting this test was to examine the ubiquitination level of SIRT1 in MC3T3-E1 cells treated with si-USP14, MG132, or both. The experiments were conducted in 6-well plates with 5×10^5 cells per well of MC3T3-E1 cells. Cells were cultured for a duration of 48 h under standard conditions. Following the manufacturer's protocol, we used an immunoprecipitation kit (catalog number PK10008, Proteintech). Briefly, cell lysates were prepared using RIPA buffer (catalog number 9806, Cell Signaling Technology). Each sample was incubated with SIRT1 antibody (1:200, catalog number 13161-1-AP, proteintech, USA) overnight at 4 °C. Protein A/G agarose beads (catalog number 16–266, EMD Millipore) were then added and incubated at 4 °C for 4 h. The bead-antibody-antigen complexes were collected by centrifugation and washed four times with cold lysis buffer. Finally, immunoprecipitated proteins were analyzed by Western blot that was probed with an anti-ubiquitin (Ub) antibody (1:5000, catalog number ab134953, Abcam, Shanghai, China) to examine the ubiquitination level.

Data analysis

SPSS 21.0 software was used for data analysis (IBM, USA). Quantitative data were presented as $\bar{x} \pm s$, and GraphPad 9.0 (GraphPad Software, USA) was used for plotting. Group comparisons were performed using paired t-tests, and multiple group comparisons were performed using one-way ANOVA followed by Tukey's post hoc test. A p value less than 0.05 was considered statistically significant. All experiments were independently repeated at least three times.

Results

Low expression of USP14 and SIRT1 in bone tissue of patients with osteomyelitis fractures

First, we examined the expression of USP14 in bone tissue from patients with combined osteomyelitis fractures and healthy fractures caused by trauma. As shown in Fig. 1A by RT-qPCR, the expression of USP14 in bone tissue from patients with combined osteomyelitis fractures was significantly decreased compared to that in bone tissue from patients with healthy fractures caused by trauma ($p < 0.001$). Western blot results also indicated an apparent decrease in the expression of USP14 in bone tissue from combined osteomyelitis fractures ($p < 0.001$) (Fig. 1B). We then examined the SIRT1 level in combined osteomyelitis fractures and healthy fractures caused by trauma by RT-qPCR. As shown in Fig. 1C, the expression of SIRT1 in bone tissue from patients with combined osteomyelitis fractures was found to be decreased compared to healthy fractures caused by traumatic bone tissue ($p < 0.05$). Similarly, Western blot results indicated a significant decrease in SIRT1 protein levels in bone tissue from patients with combined osteomyelitis fractures compared to bone tissue from healthy fractures caused by trauma ($p < 0.001$) (Fig. 1D). Importantly, the levels of SIRT1 protein in bone tissue of patients with combined osteomyelitis fractures were significantly lower than the levels of SIRT1 mRNA. These results suggest a decreased USP14 and SIRT1 in bone tissue of patients with osteomyelitis fractures.

Isolation and identification of BMSCs-exo

Exosomes are the main paracrine forms of BMSCs, and BMSCs-exo were obtained from BMSCs based on well-established extraction and isolation methods. Firstly, we observed the growth morphology of BMSCs and their ability to undergo osteogenic and adipogenic differentiation using an optical microscope. As shown in Figs. 2A-C, the BMSCs exhibited spindle-shaped morphology and grew in parallel or vortex patterns (Fig. 2A). Meanwhile, these BMSCs differentiated into osteoblasts under osteogenic differentiation induction culture (Fig. 2B) and into adipocytes under adipogenic differentiation induction culture (Fig. 2C), suggesting the successful cultivation of BMSCs. Subsequently, exosomes derived from BMSCs were isolated by ultracentrifugation and then characterized using TEM and Western blot. TEM observation of exosome morphology showed that most of the exosomes had a cup-like shape with varying sizes (Fig. 2D). Western blot analysis showed that exosome-specific marker proteins were clearly expressed, while Calnexin was not detected (negatively expressed) in BMSCs-exo (Fig. 2E). These findings suggest that exosomes were successfully isolated from BMSCs.

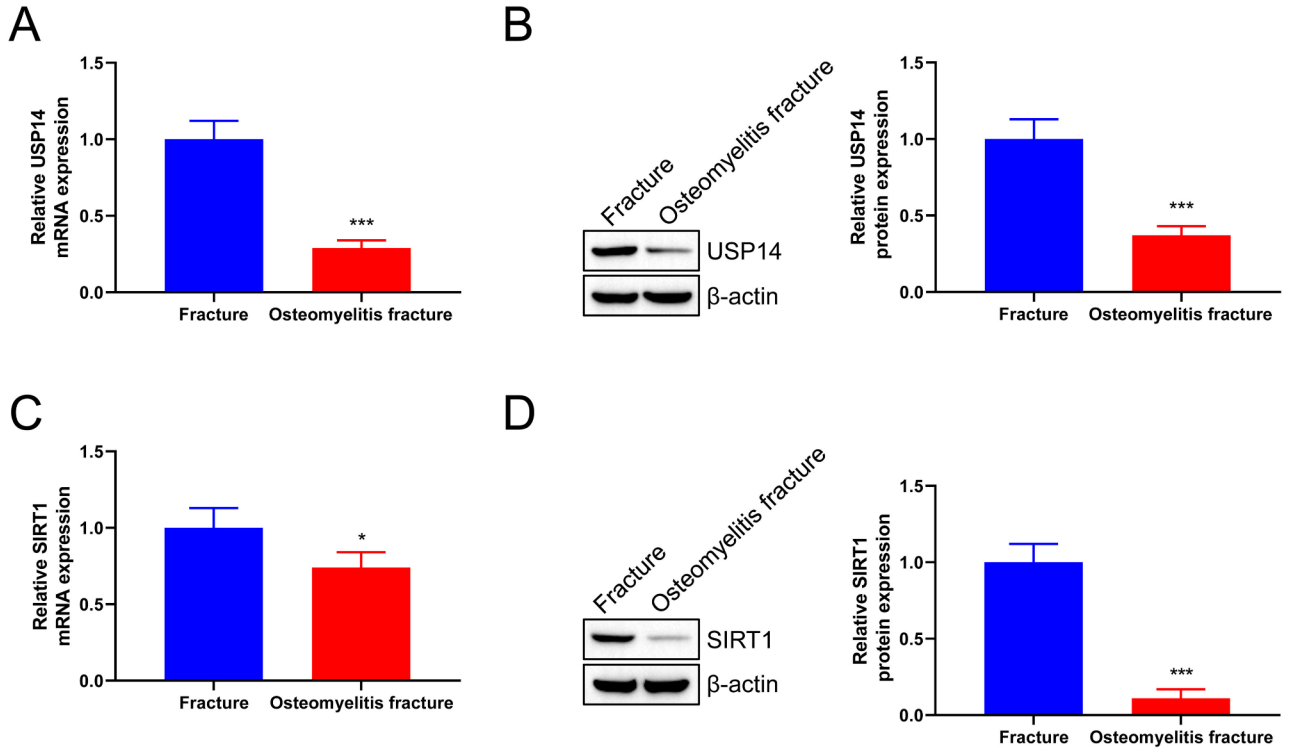

Fig. 1 Low expression of USP14 and SIRT1 in bone tissue of patients with osteomyelitis fractures. **A** and **C**. RT-qPCR detection of USP14 and SIRT1 expression in bone tissue of patients with fractures and those with concurrent osteomyelitis fractures. **B** and **D**. Western blot detection of USP14 and SIRT1 expression in bone tissue of patients with fractures and those with concurrent osteomyelitis fractures. $^{*}P<0.05$, $^{***}P<0.001$ vs. Fracture group

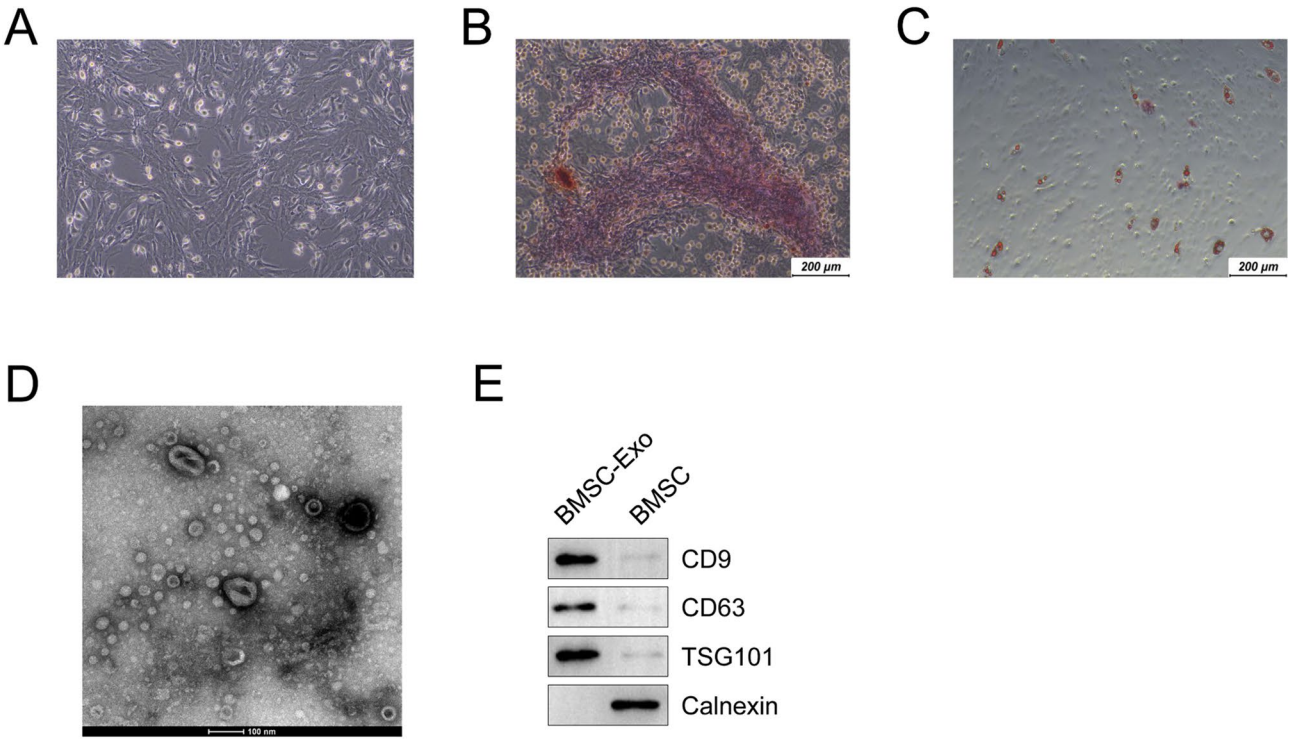

Fig. 2 Isolation and identification of BMSCs-exo. (**A**) Morphology of BMSCs was observed under optical microscope. (**B**) Alizarin Red S staining was used to detect osteogenic differentiation ability of BMSCs. (**C**) Oil Red O staining was performed to detect adipogenic differentiation ability of BMSCs. (**D**) TEM observation of exosome morphology. (**E**) Western blot detection of exosome-specific markers (CD9, CD63, and TSG101) and Calnexin expression

Silencing of USP14 blocked the promoting effect of BMSCs-exo on SIRT1 protein in the cell model of osteomyelitis

We established an in vitro model of osteomyelitis induced by S. aureus in MC3T3-E1 cells. First, we transfected BMSCs with either USP14 overexpression or USP14 knockdown. Figure 3A indicated successful construction of overexpressed and silenced BMSCs for USP14 ($p < 0.001$). Subsequently, BMSCs-exo were isolated after overexpression and knockdown of UPS14 in BMSCs. RT-qPCR findings indicated that USP14 overexpression promoted the expression of USP14 mRNA in BMSCs-exo ($p < 0.001$), while USP14 knockdown inhibited its expression ($p < 0.001$) (Fig. 3B). However, such changes were not evident at the USP14 protein level, as shown in Fig. 3C. Next, we co-cultured MC3T3-E1 cells with BMSCs-exo transfected with USP14 overexpressing or knockdown. As shown in Figs. 3D-F, in the S. aureus-induced osteomyelitis model, the mRNA and protein levels of USP17 and SIRT1 were significantly lower in MC3T3-E1 cells compared to controls ($p < 0.05$, $p < 0.001$). Treating uninduced MC3T3-E1 cells with BMSCs-exo significantly increased these levels, with SIRT1 protein showing more

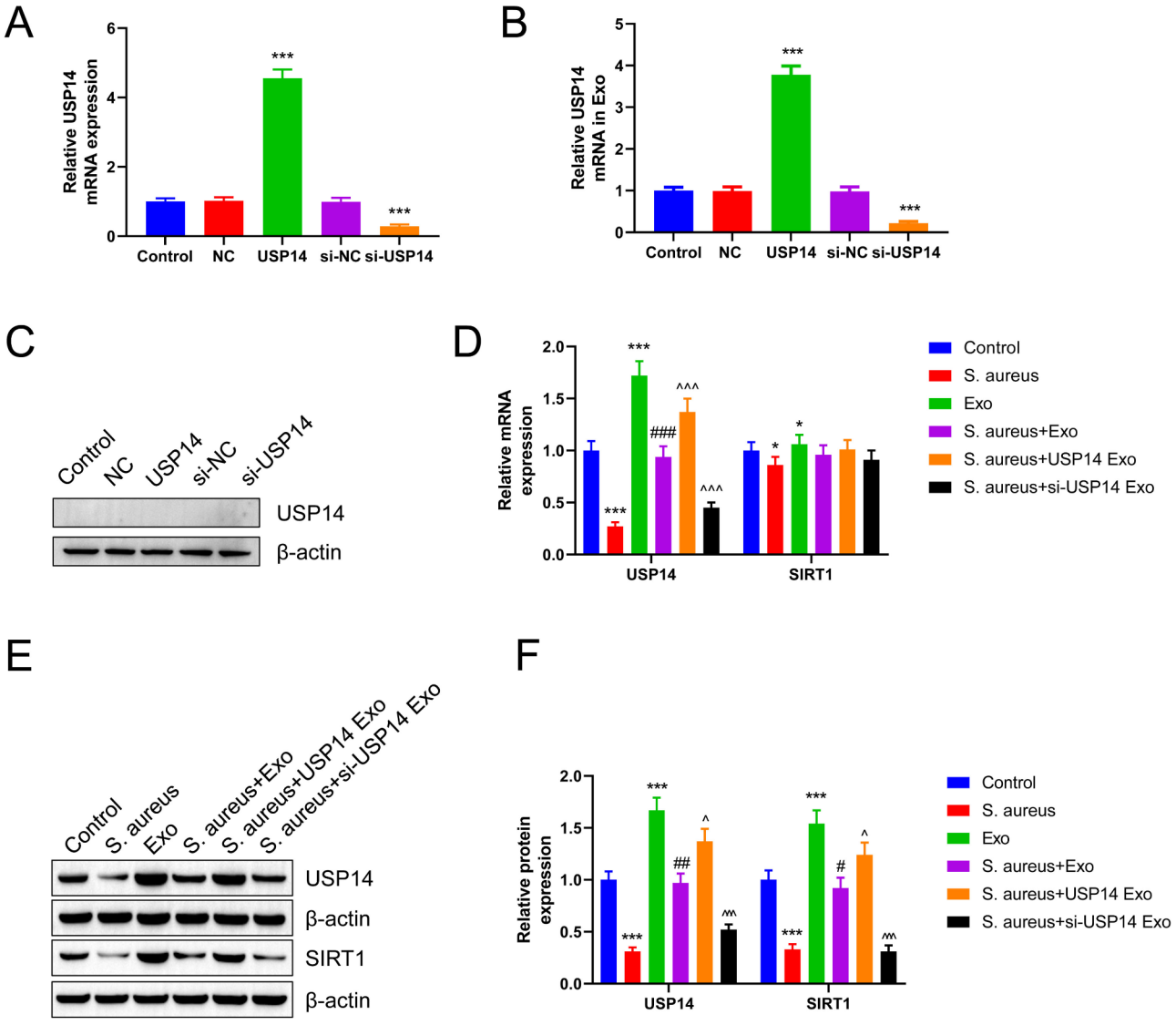

Fig. 3 Silencing of USP14 blocked the promoting effect of BMSCs-exo on SIRT1 protein in the cell model of osteomyelitis. We transfected BMSCs with either OE-USP14 or si-USP14. (**A**) RT-qPCR detection of the transfection efficiency of OE-USP14 or si-USP14 in BMSCs. (**B**) RT-qPCR detection of USP14 mRNA expression in BMSCs-exo with overexpression or knockdown of USP14. (**C**) Western blot detection of USP14 protein expression levels in BMSCs-exo with overexpression or knockdown of USP14. S. aureus induced osteomyelitis model. These BMSCs-exo transfected with OE-USP14 or si-USP14 were co-cultured with S. aureus-treated MC3T3-E1 cells. (**D**) RT-qPCR detection of USP14 and SIRT1 mRNA expression levels in MC3T3-E1 cells. **(E-F)** Western blot detection of USP14 and SIRT1 protein expression levels in MC3T3-E1 cells. $^{*}P < 0.05$, $^{***}P < 0.001$ vs. NC group or si-NC group or control group; $^{\#}P < 0.05$, $^{\#\#}P < 0.01$, $^{\#\#\#}P < 0.001$ vs. S. aureus group; $^{\wedge}P < 0.05$, $^{\wedge\wedge\wedge}P < 0.001$ vs. S. aureus + Exo group

pronounced changes than its mRNA ($p < 0.05$, $p < 0.001$). In the osteomyelitis cell model, BMSCs-exo treatment significantly promoted USP14 and SIRT1 expression (mRNA and protein) ($p < 0.05$, $p < 0.01$, $p < 0.001$). This effect was enhanced when using BMSCs-exo overexpressing USP14 ($p < 0.05$, $p < 0.001$), but suppressed in groups treated with BMSCs-exo where USP14 was knocked down ($p < 0.001$). Notably, SIRT1 mRNA levels remained unaffected regardless of whether BMSCs-exo overexpressed or knocked down USP14, suggesting that USP14 regulated SIRT1 protein post-transcriptionally rather than through mRNA modulation. In conclusion, the results showed that suppressing USP14 hindered the enhancement of SIRT1 protein by BMSCs-exo, while increasing USP14 levels amplified the stimulating impact of BMSCs-exo on SIRT1 protein in the osteomyelitis cell model.

Silencing USP14 hampered the osteogenic differentiation-promoting effect of BMSCs-exo in osteomyelitis

Subsequently, we evaluated the interference of USP14 on BMSCs-exo on the effect of osteogenic differentiation in the osteomyelitis cell model. The results of the CCK-8 assay showed that treatment with BMSCs-exo significantly enhances the viability of MC3T3-E1 cells after S. aureus treatment ($p < 0.001$), with a more pronounced effect observed in MC3T3-E1 cells that were treated with BMSCs-exo with overexpressed USP14 ($p < 0.001$) and a significant reduction in viability observed in MC3T3-E1 cells treated with BMSCs-exo silencing USP14 ($p < 0.001$) (Fig. 4A). Furthermore, our findings revealed that the administration of BMSCs-exo led to decreased levels of IL-6 and TNF-α in the osteomyelitis cell model ($p < 0.001$). This effect was particularly prominent in the group treated with BMSCs-exo overexpressing USP14 ($p < 0.001$). Conversely, elevated levels of IL-6 and TNF-α were observed in MC3T3-E1 cells treated with BMSCs-exo with USP14 knocked down ($p < 0.001$) (Fig. 4B). Meanwhile, ALP staining analysis revealed that treatment with BMSCs-exo significantly enhances the osteogenic differentiation of MC3T3-E1 cells post S. aureus treatment. This enhancement was especially notable in cells treated with BMSCs-exo overexpressing USP14. Conversely, a significant reduction in osteogenic differentiation was observed in cells treated with BMSCs-exo where USP14 was knocked down (Fig. 4C). Notably, the expression levels of osteogenic differentiation markers RUNX2 and OCN were markedly increased in the BMSCs-exo group ($p < 0.01$). This effect was more remarkable in BMSCs-exo of overexpressing USP14 group ($p < 0.05$), while it was significantly reversed in BMSCs-exo silencing USP14 group ($p < 0.01$, $p < 0.001$) (Fig. 4D).

USP14 regulates the deubiquitination of SIRT1 in MC3T3-E1 cells

Next, we investigated the role of USP14 in the ubiquitination of SIRT1. Figure 5A indicated the successful transfection of si-UPS14 in MC3T3-E1 cells ($p < 0.001$). Subsequently, we assessed the impact of USP14 knockdown on SIRT1 expression in MC3T3-E1 cells. The findings revealed that both USP14 knockdown and treatment with the proteasome inhibitor MG132 did not have a significant effect on SIRT1 mRNA expression in MC3T3-E1 cells (Fig. 5B). And, USP14 knockdown significantly inhibits the expression of SIRT1 at the protein level in MC3T3-E1 cells ($p < 0.001$), and this trend is reversed upon the addition of the proteasome inhibitor MG132 ($p < 0.001$) (Fig. 5C). Additionally, CO-IP assay results indicated that the level of ubiquitination of SIRT1 was elevated in cells transfected with si-USP14 alone or after the addition of MG132 alone, and was higher in cells transfected with si-USP4 after supplementation with MG132. Regarding the Co-IP technique, IP is used to isolate SIRT1 and its interacting partners. The two bands might represent different forms of ubiquitinated SIRT1, such as different ubiquitination degrees or conformations. The increasing trend of SIRT1 ubiquitination has implications. The elevation in cells with si-USP4 alone suggests USP14 may suppress SIRT1 ubiquitination normally. With MG132 alone, the increase indicates the proteasome-mediated degradation pathway may regulate Sirt1 ubiquitination. The combined treatment resulting in the highest level implies USP14 and this pathway may interactively regulate SIRT1 ubiquitination. Specifically, IP isolated SIRT1 and associated proteins, while immunoblotting (IB) detected ubiquitinated SIRT1, confirming the protective role of USP14 against SIRT1 degradation in MC3T3-E1 cells (Fig. 5D). These results suggest that USP14 inhibits the ubiquitination degradation of SIRT1 and enhances the activity of Sirt1 in MC3T3-E1 cells.

Overexpression of USP14 regulates SIRT1 deubiquitination in MC3T3-E1 cells

Finally, MC3T3-E1 cells were transfected with the OE-NC or OE-USP14. The relative protein expression levels of USP14 were significantly increased in cells transfected with OE-USP14 compared to the NC group ($p < 0.001$) (Fig. 6A). RT-qPCR analysis revealed that overexpression of USP14 did not significantly affect the mRNA levels of SIRT1 (Fig. 6B). However, Western blot analysis showed that overexpression of USP14 significantly increased the protein levels of SIRT1 compared to the NC group ($p < 0.001$) (Fig. 6C). To further investigate the effect of USP14 on SIRT1 ubiquitination, we performed IP followed by IB analysis. The results indicated that overexpression of USP14 led to a significant decrease in SIRT1 ubiquitination levels compared to the NC group

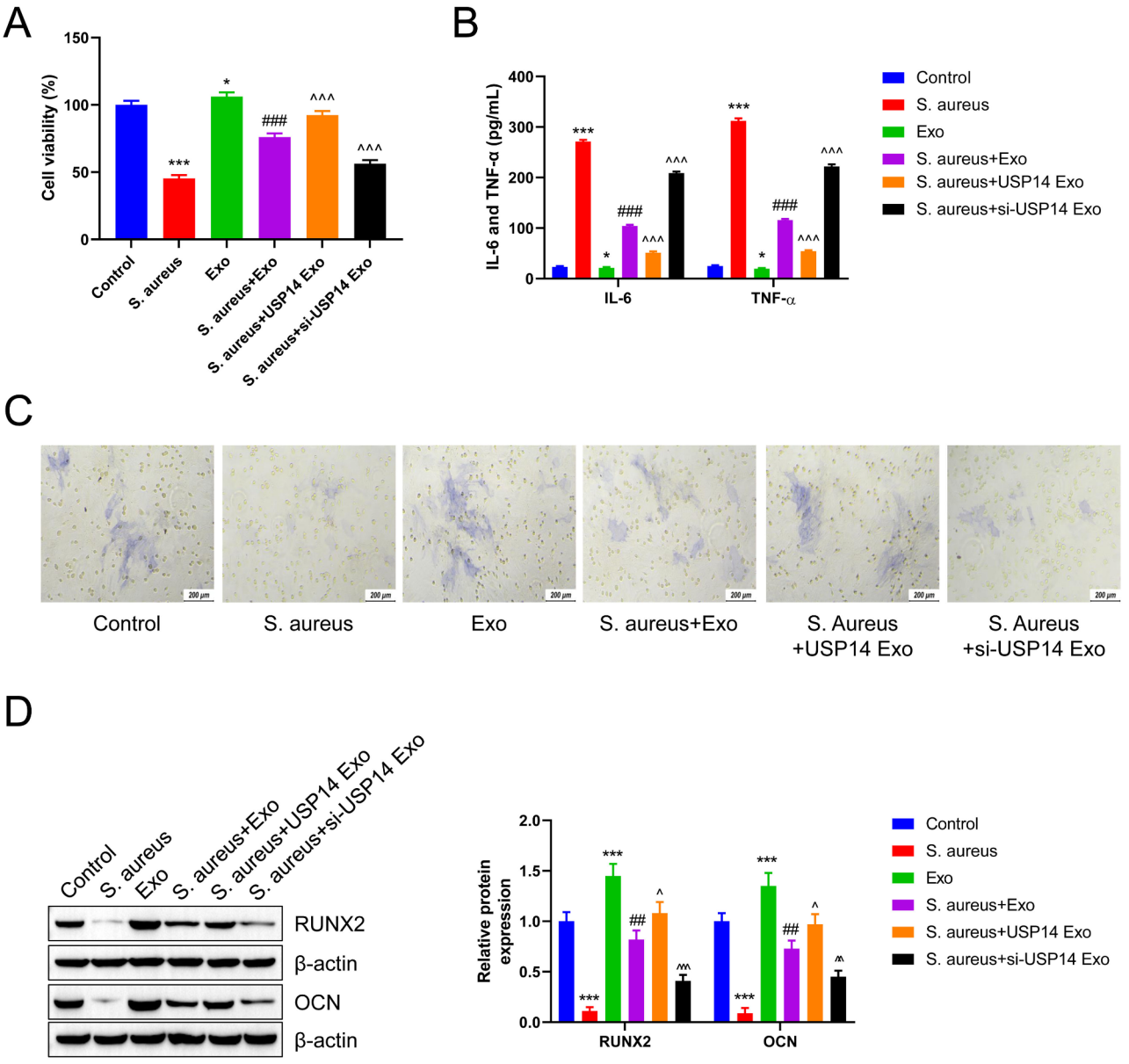

Fig. 4 Silencing USP14 hampered the osteogenic differentiation-promoting effect of BMSCs-exo in osteomyelitis. S. aureus induced osteomyelitis model. BMSCs-exo transfected with OE-USP14 or si-USP14 were co-cultured with S. aureus-treated MC3T3-E1 cells. (**A**) CCK-8 assay was used to evaluate cell viability of MC3T3-E1 cells. (**B**) ELISA detection of IL-6 and TNF-α levels in the supernatant of different groups of MC3T3-E1 cells. (**C**) ALP staining was performed to evaluate osteogenic differentiation of MC3T3-E1 cells. (**D**) Western blot detection of osteogenic differentiation markers RUNX2 and OCN expression. *$P<0.05$, ***$P<0.001$ vs. Control group; $^{\#\#}P<0.01$, $^{\#\#\#}P<0.001$ vs. S. aureus group; $^{\wedge}P<0.05$, $^{\wedge\wedge}P<0.01$, $^{\wedge\wedge\wedge}P<0.001$ vs. S. aureus + Exo group

(Fig. 6D). These findings suggest that overexpression of USP14 promoted SIRT1 protein levels and reduced its ubiquitination in MC3T3-E1 cells, potentially contributing to the regulation of SIRT1 stability and function.

Discussion

Post-traumatic osteomyelitis following a fracture is a problematic condition [33, 34]. Due to its unusually complex conditions, the treatment of post-traumatic osteomyelitis is challenging, as it involves significant difficulties, long duration, and a high risk of disability. The treatment of this disease has always been a major clinical challenge [35]. Research has shown that inflammation is an important pathological change in the progression of osteomyelitis [2]. Multiple researches showed BMSCs have a very important function in bone tissue repair and regeneration by regulating inflammation, osteogenic differentiation, and angiogenesis through paracrine mechanisms [36–38]. In this study, we focused on exploring the key roles and underlying molecular mechanisms of BMSCs-exo in osteomyelitis.

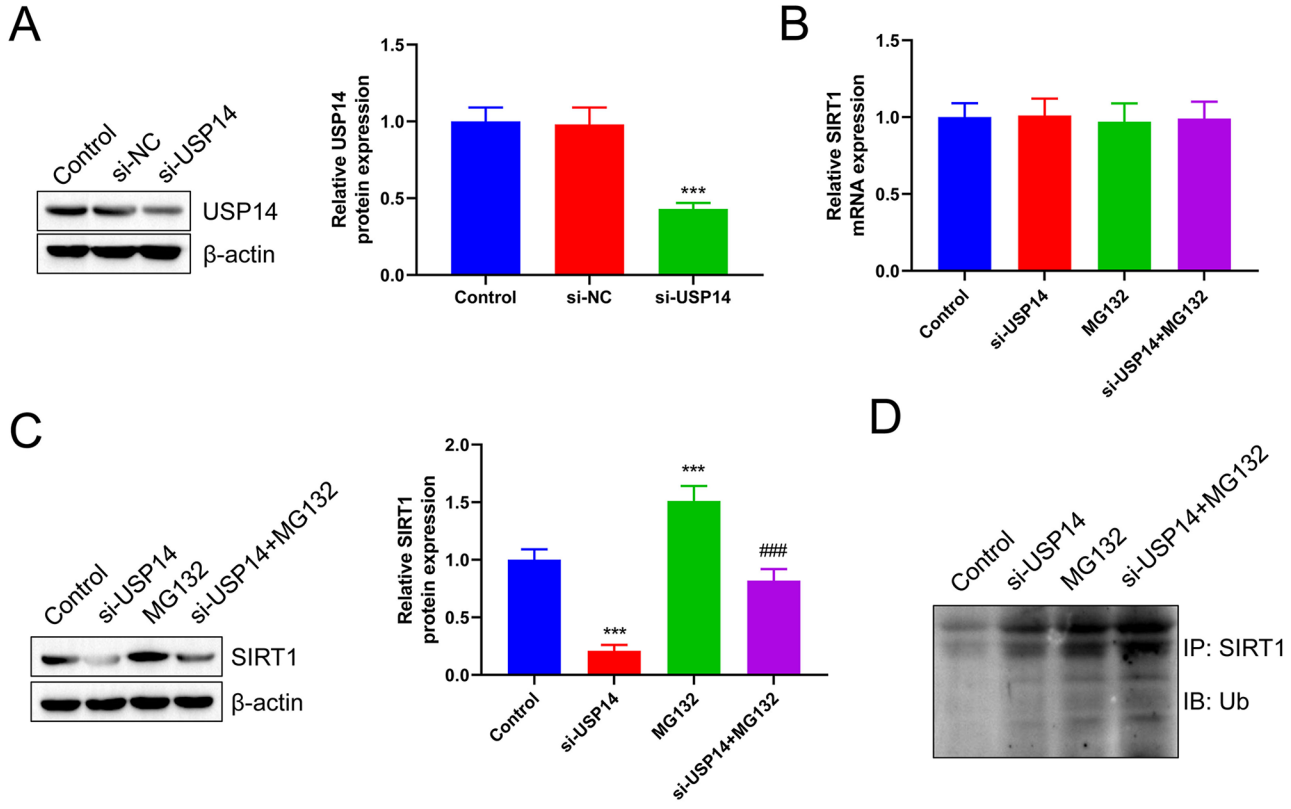

Fig. 5 USP14 regulates the deubiquitination of SIRT1 in MC3T3-E1 cells. si-NC or si-USP14 was transfected into MC3T3-E1 cells, which were then either treated or not treated with MG132. (**A**) Western blot detection of USP14 transfection efficiency in MC3T3-E1 cells. (**B**) RT-qPCR detection of SIRT1 mRNA expression in MC3T3-E1 cells. MG132 or si-USP14 treated MC3T3-E1 cells or added MG132 in MC3T3-E1 cells transfected with si-USP14. (**C**) Western blot detection of SIRT1 protein expression in MC3T3-E1 cells. (**D**) Ubiquitination level was detected by immunoprecipitation with SIRT1 antibody followed by Western blot with anti-Ub antibody. $^{***}P < 0.001$ vs. Control group; $^{###}P < 0.001$ vs. si-USP14 group

As mentioned earlier, research has confirmed that BMSCs can deliver therapeutic factors to other cells in the lesion environment through secreting exosomes, thereby exerting their therapeutic effects [39]. In recent years, the application of BMSCs-exo in fracture repair and regeneration has been reported in numerous studies. For instance, the NEAT1/miR-339-5p/SPI1 axis feedback loop favors osteogenic differentiation in children with acute suppurative osteomyelitis [40]. Yang et al. [41] found that human umbilical cord mesenchymal stem cell-derived exosomes enhance osteogenic differentiation of periodontal ligament stem cells under hyperglycemic conditions by regulating the PI3K/AKT signaling pathway. The lncRNA MALAT1 carried by BMSC-secreted exosomes alleviates osteoporosis by mediating the miR-34c/SATB2 axis [42]. In our study, we found that BMSCs-exo exert a protective role in osteomyelitis by inhibiting inflammation and enhancing osteogenic differentiation, but the underlying mechanisms require further elucidation.

USP14, belonging to the ubiquitin-specific processing family, regulates various cellular activities [43, 44]. We observed USP14 was lowly expressed in bone tissues of osteomyelitis fracture patients and in the cell model of osteomyelitis in this research, suggesting that USP14 dysregulation contributes to the progression of osteomyelitis. Nevertheless, the impact of USP14 in osteomyelitis is still not well-defined. Some researchers have revealed that USP14 plays a significant role in regulating inflammation during the onset and progression of the disease. Activation of USP14 was able to stabilize the histone acetyltransferase (CBP), further regulating lung inflammation [45]. USP14 regulates LPS-induced inflammation by increasing ERK1/2 phosphorylation and NF-κB activation [46].Moreover, emerging studies have confirmed that USP14 modulates inflammation and participates in the repair of osteoarthritis [26]. In our study, we found that BMSCs-exo upregulates USP14 to inhibit inflammation and enhance cell viability and osteogenic differentiation. This result demonstrates for the first time the important role of USP14 in osteomyelitis, and reveals that USP14 serves as a crucial target for the protective effects of BMSCs-exo against osteomyelitis.

Research has shown that SIRT1 is a promising regulator of bone remodeling [47], playing a vital role in maintaining osteoblast viability, reducing bone resorption, inhibiting

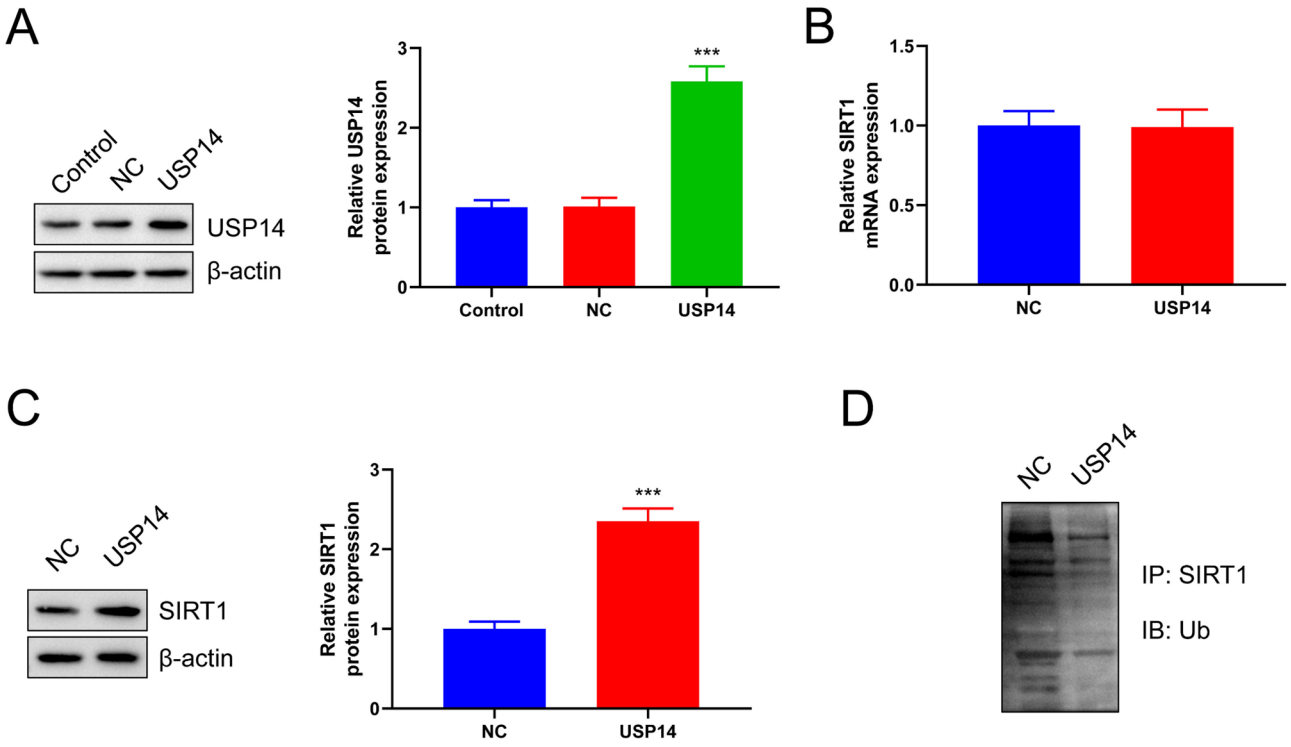

Fig. 6 Overexpression of USP14 regulates SIRT1 deubiquitination in MC3T3-E1 cells. OE-NC or OE-USP14 was transfected into MC3T3-E1 cells and designated as the NC group and USP14 group, respectively. **A**. Western blot analysis showing the relative protein expression levels of USP14 in MC3T3-E1 cells. **B**. RT-qPCR analysis of SIRT1 mRNA levels in MC3T3-E1 cells transfected with OE-NC or OE-USP14. **C**. Western blot analysis showing the relative protein expression levels of SIRT1 in MC3T3-E1 cells transfected with OE-NC or OE-USP14. **D**. IP followed by IB analysis of SIRT1 ubiquitination in MC3T3-E1 cells transfected with OE-NC or OE-USP14. IP was performed using an anti-SIRT1 antibody, and ubiquitination was detected using an anti-Ub antibody. ***$P < 0.001$ vs. Control group

osteoarthritis progression, and promoting fracture repair and regeneration [48]. SIRT1 can inhibit inflammation by regulating the expression of the osteogenic transcription activator RUNX2 in osteoarthritis chondrocytes [29]. 8-MOP enhances SIRT1 expression, inhibits NF-κB phosphorylation, and suppresses inflammatory and oxidative stress responses, thereby alleviating the progression of osteoarthritis [30].However, the impact of SIRT1 on osteomyelitis needs to be further verified. Low levels of SIRT1 expression in bone tissues of osteomyelitis fracture patients and in the cell model of osteomyelitis were found in this study, indicating that SIRT1 dysregulation also contributes to osteomyelitis progression. Interestingly, we observed that treatment with BMSCs-exo in uninduced MC3T3-E1 cells led to a significant increase in SIRT1 at both mRNA and protein levels, with the changes in SIRT1 protein being more pronounced than those at the mRNA level. However, in the osteomyelitis cell model, BMSCs-exo significantly upregulated the expression level of SIRT1 protein without having a notable impact on SIRT1 mRNA expression levels. Additionally, whether using BMSCs-exo with overexpressed USP14 or BMSCs-exo with USP14 knockdown to treat the osteomyelitis cell model, there was a significant effect on SIRT1 protein levels but no significant impact on SIRT1 mRNA expression levels. This suggests that USP14, as a key target for the protective effects of BMSCs-exo against osteomyelitis, may not directly affect SIRT1 protein expression by regulating SIRT1 mRNA levels.

SIRT1 expression is regulated by multiple layers, including ubiquitination, methylation, and phosphorylation [28]. Ubiquitination is an important post-translational modification that regulates protein stability [49]. Multiple studies have shown that various proteins regulate SIRT1 ubiquitination degradation and participate in disease progression. For example, Fyn deficiency inhibits oxidative stress by reducing SIRT1 ubiquitination, thus alleviating diabetic renal fibrosis [50]. The lncRNA-CRNDE inhibits the ubiquitination level of SIRT1 mediated by the E3 ligase SMURF2, upregulates SIRT1 protein expression, regulates BMSC chondrogenic differentiation, and promotes osteoarthritis cartilage repair [51]. As USP14 is a deubiquitinating enzyme that regulates protein deubiquitination and maintains protein activity [52], USP14 inhibits the degradation of the negative regulator of NF-κB signaling, the NOD-like receptor family caspase recruitment domain-containing protein 5 (NLRC5), thereby suppressing endothelial pro-inflammatory activation and alleviating the progression of atherosclerosis [25]. In this study, we found that si-USP14 significantly reduced

the protein levels of SIRT1 without affecting its mRNA levels and promoted the ubiquitination-mediated degradation of SIRT1. Conversely, treatment with the proteasome inhibitor MG132 prevented the degradation of ubiquitinated proteins, thereby inhibiting SIRT1 ubiquitination and increasing its protein levels, while leaving its mRNA levels unaffected. When si-USP14 was combined with MG132, MG132 effectively blocked the decrease in SIRT1 protein levels induced by si-USP14. Additionally, overexpression of USP14 significantly increased SIRT1 protein levels, suppressed its ubiquitination, but did not alter its mRNA levels. These findings indicate that USP14 regulates SIRT1 protein expression through post-transcriptional mechanisms rather than via modulation of mRNA levels. Specifically, USP14 controls SIRT1 expression in MC3T3-E1 cells by regulating the ubiquitination-mediated degradation of SIRT1. In summary, our results highlight the critical role of USP14 in maintaining SIRT1 protein stability and underscore its importance in regulating SIRT1 protein expression by modulating SIRT1 ubiquitination. This provides new insights into the potential mechanisms by which USP14 may contribute to the treatment of osteomyelitis.

Conclusion

Our results demonstrate that BMSCs-exo exert a protective role in traumatic osteomyelitis by inhibiting inflammation and promoting osteogenic differentiation. Mechanistically, BMSCs-exo upregulate the expression of USP14 in osteoblasts, potentially associated with SIRT1 deubiquitination. However, future research should focus on elucidating the detailed molecular mechanisms of BMSCs-exo-mediated delivery of USP14 and its long-term effects on osteomyelitis treatment. In vivo studies are also needed to validate these findings and explore the therapeutic potential in preclinical models, which is crucial for translating these promising results into clinical applications.

Abbreviations

BMSCs	Bone marrow mesenchymal stem cells
BMSCs-exo	Exosomes derived from bone marrow mesenchymal stem cells
S. aureus	Staphylococcus aureus
UPS	Ubiquitin-proteasome system
USP14	Ubiquitin-specific protease 14
SIRT1	Sirtuin 1
TEM	Transmission electron microscopy
CCK-8 assay	Cell Counting Kit-8 assay
ELISA assay	Enzyme-Linked Immunosorbent Assay
RT-qPCR	Reverse transcription polymerase chain reaction
Co-IP	Co-immunoprecipitation
IB	Immunoblotting
OE-NC	Overexpression negative control
OE-USP17	Overexpression plasmid USP14
Si-NC	Small interfering RNA negative control
Si-USP7	Small interfering RNA targeting USP14
Ub	Ubiquitin
LPS	Lipopolysaccharides
FBS	Fetal bovine serum
PBS	Phosphate-buffered saline

Author contributions

Jun Yu is responsible for Methodology, Investigation, Data curation and original draft. Ming Yang, Yun Jin and Kaijie Yang are also responsible for Methodology, Investigation, Data curation and original draft. Haibo Yang is in charge of Writing, review and editing.

Funding

Ningxia Natural Science Foundation (2024AAC03629).

Data availability

The datasets used during the present study are available from the corresponding author upon reasonable request. All the data obtained in the current study were available from the corresponding authors on reasonable request.

Declarations

Ethical approval

This study was approved by the Ethics Committee of General Hospital of Ningxia Medical University (approved number: KYLL-2023-0310). Furthermore, the study was conducted in strict accordance with the Declaration of Ethical Principles of Medical Research Involving Human Subjects in Helsinki.

Consent to participate

All the participants agreed to the publication of the manuscript.

Competing interests

The authors declare no competing interests.

Received: 25 December 2024 / Accepted: 6 May 2025
Published online: 29 May 2025

References

1. Lew DP, Waldvogel FA, Osteomyelitis. Lancet. 2004;364(9431):369–79.
2. Bury DC, Rogers TS, Dickman MM. Osteomyelitis: diagnosis and treatment. Am Fam Physician. 2021;104(4):395–402.
3. Simona B, Rocco P, Laura R, Alessandro S, Nicola M, Vincenzo D. Effect of pulsed electromagnetic fields on human osteoblast cultures. Physiother Res Int. 2012;18(2).
4. Mangiavini L, Peretti G, Canciani B, Maffulli N. Epidermal growth factor signalling pathway in endochondral ossification: an evidence-based narrative review. Ann Med. 2022;54(1):37–50.
5. Lassoued Ferjani H, Makhlouf Y, Maatallah K, Triki W, Ben Nessib D, Kaffel D, et al. Management of chronic recurrent multifocal osteomyelitis: review and update on the treatment protocol. Expert Opin Biol Ther. 2022;22(6):781–7.
6. Chinzorig T, Beguesse KA, Canoville A, Phillips G, Zanno LE. Chronic fracture and osteomyelitis in a large-bodied ornithomimosaur with implications for the identification of unusual endosteal bone in the fossil record. Anat Rec (Hoboken). 2023;306(7):1864–79.
7. Urish KL, Cassat JE. Staphylococcus aureus osteomyelitis: bone, Bugs, and surgery. Infect Immun. 2020;88(7).
8. Zaineb AFA, Narsimha RP, Shobanbabu B, Ginell RP, Mark SS, Peter AC. Evaluation of bone and kidney toxicity of BT2-peg2, a potential carrier for the targeted delivery of antibiotics to bone. Toxicol Rep. 2021;8(0).
9. Alexandra S, Ufuk E, Aphrodite V, Ioanna M, Ioannis K. Defining the most potent osteoinductive culture conditions for MC3T3-E1 cells reveals no implication of oxidative stress or energy metabolism. Int J Mol Sci. 2024;25(8).
10. Xinkun S, Wenjia H, Linchao P, Chongxing L, Lili Y, Zhennan D et al. Antibacterial and osteogenic functionalization of titanium with Silicon/Copper-Doped High-Energy shot Peening-Assisted Micro-Arc oxidation technique. Front Bioeng Biotechnol. 2020;8(0).
11. Tingting S, Kai H. Network Pharmacology-Based analysis on Lonicera japonica for chronic osteomyelitis treatment. J Oncol. 2022;2022:0.
12. Wei Z, Yiwei L, Yang Z, Xin M, Chaolai J, Haojie S et al. Staphylococcus aureus infection initiates Hypoxia-Mediated transforming growth Factor-β1 upregulation to trigger osteomyelitis. mSystems. 2022;7(4).
13. Fischer V, Haffner-Luntzer M. Interaction between bone and immune cells: implications for postmenopausal osteoporosis. Semin Cell Dev Biol. 2022;123:14–21.

14. Wang X, Wang Y, Gou W, Lu Q, Peng J, Lu S. Role of mesenchymal stem cells in bone regeneration and fracture repair: a review. Int Orthop. 2013;37(12):2491–8.
15. Alessio GV, Mary BM, Laura dG, Enrico R, Francesco O, Nicola M. Making them commit: strategies to influence phenotypic differentiation in mesenchymal stem cells. Sports Med Arthrosc Rev. 2018;26(2).
16. Alasdair Gawain K, Tina Patricia D, Khondoker Mehedi A, Param M, Karen H, Nicola M et al. BMP2 repression and optimized culture conditions promote human bone marrow-derived mesenchymal stem cell isolation. Regen Med. 2015;10(2).
17. Li W, Li L, Cui R, Chen X, Hu H, Qiu Y. Bone marrow mesenchymal stem cells derived Exosomal Lnc TUG1 promotes bone fracture recovery via miR-22-5p/Anxa8 axis. Hum Cell. 2023;36(3):1041–53.
18. Cai B, Lin D, Li Y, Wang L, Xie J, Dai T, et al. N2-Polarized neutrophils guide bone mesenchymal stem cell recruitment and initiate bone regeneration: A missing piece of the bone regeneration puzzle. Adv Sci (Weinh). 2021;8(19):e2100584.
19. Chen BY, Sung CW, Chen C, Cheng CM, Lin DP, Huang CT, et al. Advances in exosomes technology. Clin Chim Acta. 2019;493:14–9.
20. Liu H, Li R, Liu T, Yang L, Yin G, Xie Q. Immunomodulatory effects of mesenchymal stem cells and mesenchymal stem Cell-Derived extracellular vesicles in rheumatoid arthritis. Front Immunol. 2020;11:1912.
21. Wang Y, Chen W, Zhao L, Li Y, Liu Z, Gao H, et al. Obesity regulates miR-467/HoxA10 axis on osteogenic differentiation and fracture healing by BMSC-derived exosome LncRNA H19. J Cell Mol Med. 2021;25(3):1712–24.
22. Shen X, Qin J, Wei Z, Liu F. Bone marrow mesenchymal stem cell exosome-derived LncRNA TUC339 influences the progression of osteoarthritis by regulating synovial macrophage polarization and chondrocyte apoptosis. Biomed Pharmacother. 2023;167:115488.
23. Cockram PE, Kist M, Prakash S, Chen SH, Wertz IE, Vucic D. Ubiquitination in the regulation of inflammatory cell death and cancer. Cell Death Differ. 2021;28(2):591–605.
24. Sippl W, Collura V, Colland F. Ubiquitin-specific proteases as cancer drug targets. Future Oncol. 2011;7(5):619–32.
25. Fu Y, Qiu J, Wu J, Zhang L, Wei F, Lu L, et al. USP14-mediated NLRC5 upregulation inhibits endothelial cell activation and inflammation in atherosclerosis. Biochim Biophys Acta Mol Cell Biol Lipids. 2023;1868(5):159258.
26. Li M, Zhao J, Jia L. USP14-mediated IκBα degradation exacerbates NF-κB activation and IL-1β-stimulated chondrocyte dedifferentiation. Life Sci. 2019;218:147–52.
27. Shan H, Li X, Ouyang C, Ke H, Yu X, Tan J, et al. Salidroside prevents PM2.5-induced BEAS-2B cell apoptosis via SIRT1-dependent regulation of ROS and mitochondrial function. Ecotoxicol Environ Saf. 2022;231:113170.
28. Yang Y, Liu Y, Wang Y, Chao Y, Zhang J, Jia Y, et al. Regulation of SIRT1 and its roles in inflammation. Front Immunol. 2022;13:831168.
29. Terauchi K, Kobayashi H, Yatabe K, Yui N, Fujiya H, Niki H et al. The NAD-Dependent Deacetylase Sirtuin-1 Regulates the Expression of Osteogenic Transcriptional Activator Runt-Related Transcription Factor 2 (Runx2) and Production of Matrix Metalloproteinase (MMP)-13 in Chondrocytes in Osteoarthritis. Int J Mol Sci. 2016;17(7).
30. Li J, Zhang Z, Qiu J, Huang X. 8-Methoxypsoralen has Anti-inflammatory and antioxidant roles in osteoarthritis through SIRT1/NF-κB pathway. Front Pharmacol. 2021;12:692424.
31. Ma J, Wang Z, Zhao J, Miao W, Ye T, Chen A. Resveratrol attenuates lipopolysaccharides (LPS)-Induced Inhibition of osteoblast differentiation in MC3T3-E1 cells. Med Sci Monit. 2018;24:2045–52.
32. Zhang W, Lin Y, Zong Y, Ma X, Jiang C, Shan H, et al. Staphylococcus aureus infection initiates Hypoxia-Mediated transforming growth Factor-β1 upregulation to trigger osteomyelitis. mSystems. 2022;7(4):e0038022.
33. Peng J, Ren Y, He W, Li Z, Yang J, Liu Y, et al. Epidemiological, clinical and Microbiological characteristics of patients with Post-Traumatic osteomyelitis of limb fractures in Southwest China: A Hospital-Based study. J Bone Jt Infect. 2017;2(3):149–53.
34. Alvares PA, Mimica MJ. Osteoarticular infections in pediatrics. J Pediatr (Rio J). 2020;96(1):58–64.
35. Wang X, Zhang M, Zhu T, Wei Q, Liu G, Ding J. Flourishing antibacterial strategies for osteomyelitis therapy. Adv Sci (Weinh). 2023;10(11):e2206154.
36. Li Z, Zhang B, Shang J, Wang Y, Jia L, She X, et al. Diabetic and nondiabetic BMSC-derived exosomes affect bone regeneration via regulating miR-17-5p/SMAD7 axis. Int Immunopharmacol. 2023;125(Pt B):111190.
37. Xu T, Hua Y, Mei P, Zeng D, Jiang S, Liao C. Black phosphorus thermosensitive hydrogels loaded with bone marrow mesenchymal stem cell-derived exosomes synergistically promote bone tissue defect repair. J Mater Chem B. 2023;11(20):4396–407.
38. Wu D, Chang X, Tian J, Kang L, Wu Y, Liu J, et al. Bone mesenchymal stem cells stimulation by magnetic nanoparticles and a static magnetic field: release of Exosomal miR-1260a improves osteogenesis and angiogenesis. J Nanobiotechnol. 2021;19(1):209.
39. Liu L, Liu Y, Feng C, Chang J, Fu R, Wu T, et al. Lithium-containing biomaterials stimulate bone marrow stromal cell-derived Exosomal miR-130a secretion to promote angiogenesis. Biomaterials. 2019;192:523–36.
40. Zhu D, Zhu Z, Qi H. NEAT1/microRNA 339-5p/SPI1 Axis feedback loop contributes to osteogenic differentiation in acute suppurative osteomyelitis in children. J Inflamm Res. 2023;16:2675–87.
41. Yang S, Zhu B, Tian XY, Yu HY, Qiao B, Zhao LS, et al. Exosomes derived from human umbilical cord mesenchymal stem cells enhance the osteoblastic differentiation of periodontal ligament stem cells under high glucose conditions through the PI3K/AKT signaling pathway. Biomed Environ Sci. 2022;35(9):811–20.
42. Yang X, Yang J, Lei P, Wen T. LncRNA MALAT1 shuttled by bone marrow-derived mesenchymal stem cells-secreted exosomes alleviates osteoporosis through mediating microRNA-34c/SATB2 axis. Aging. 2019;11(20):8777–91.
43. Moghadami AA, Aboutalebi Vand Beilankouhi E, Kalantary-Charvadeh A, Hamzavi M, Mosayyebi B, Sedghi H, et al. Inhibition of USP14 induces ER stress-mediated autophagy without apoptosis in lung cancer cell line A549. Cell Stress Chaperones. 2020;25(6):909–17.
44. Han KH, Kwak M, Lee TH, Park MS, Jeong IH, Kim MJ et al. USP14 inhibition regulates tumorigenesis by inducing autophagy in lung Cancer in vitro. Int J Mol Sci. 2019;20(21).
45. Wei J, Dong S, Bowser RK, Khoo A, Zhang L, Jacko AM et al. Regulation of the ubiquitylation and deubiquitylation of CREB-binding protein modulates histone acetylation and lung inflammation. Sci Signal. 2017;10(483).
46. Liu N, Kong T, Chen X, Hu H, Gu H, Liu S, et al. Ubiquitin-specific protease 14 regulates LPS-induced inflammation by increasing ERK1/2 phosphorylation and NF-κB activation. Mol Cell Biochem. 2017;431(1–2):87–96.
47. Chen Y, Zhou F, Liu H, Li J, Che H, Shen J, et al. SIRT1, a promising regulator of bone homeostasis. Life Sci. 2021;269:119041.
48. Zheng ZY, Jiang T, Huang ZF, Chu B, Gu J, Zhao X, et al. Fatty acids derived from apoptotic chondrocytes fuel macrophages FAO through MSR1 for facilitating BMSCs osteogenic differentiation. Redox Biol. 2022;53:102326.
49. Popovic D, Vucic D, Dikic I. Ubiquitination in disease pathogenesis and treatment. Nat Med. 2014;20(11):1242–53.
50. Li S, Lin Z, Xiao H, Xu Z, Li C, Zeng J, et al. Fyn deficiency inhibits oxidative stress by decreasing c-Cbl-mediated ubiquitination of Sirt1 to attenuate diabetic renal fibrosis. Metabolism. 2023;139:155378.
51. Shi C, Zheng W, Wang J. lncRNA-CRNDE regulates BMSC chondrogenic differentiation and promotes cartilage repair in osteoarthritis through SIRT1/SOX9. Mol Cell Biochem. 2021;476(4):1881–90.
52. Wang F, Ning S, Yu B, Wang Y. USP14: structure, function, and target Inhibition. Front Pharmacol. 2021;12:801328.

Publisher's note